# A Model for Ligand Binding to Hexacoordinate Hemoglobins†

James T. Trent III, Angela N. Hvitved, and Mark S. Hargrove*

*Department of Biochemistry, Biophysics, & Molecular Biology, Iowa State University, Ames, Iowa 50011*

*Received January 11, 2001; Revised Manuscript Received March 19, 2001*

ABSTRACT: Hexacoordinate hemoglobins are heme proteins capable of reversible intramolecular coordination of the ligand binding site by an amino acid side chain from within the heme pocket. Examples of these proteins are found in many living organisms ranging from prokaryotes to humans. The nonsymbiotic hemoglobins (nsHbs) are a class of hexacoordinate heme proteins present in all plants. The nsHb from rice (rHb1) has been used as a model system to develop methods for determining rate constants characterizing binding and dissociation of the His residue responsible for hexacoordination. Measurement of these reactions exploits laser flash photolysis to initiate the reaction from the unligated, pentacoordinate form of the heme protein. A model for ligand binding is presented that incorporates the reaction following rapid mixing with the reaction starting from the pentacoordinate hemoglobin (Hb).[1] This model is based on results indicating that ligand binding to hexacoordinate Hbs is not a simple combination of competing first order (hexacoordination) and second order (exogenous ligand binding) reactions. Ligand binding following rapid mixing is a multiphasic reaction displaying time courses ranging from milliseconds to minutes. The new model incorporates a "closed", slow reacting form of the protein that is not at rapid equilibrium with the reactive conformation. It is also demonstrated that formation of the closed protein species is not dependent on hexacoordination.

Recent discoveries of new hemoglobins in archea, bacteria, protozoa, plants, and vertebrate animals demonstrates the broad diversity of these proteins and suggests that they are found in most, if not all organisms (*1*−*6*). Hemoproteins serve many physiological roles, from oxygen storage and transport to catalytic activation and signal transduction (*7*). New physiological functions will certainly be discovered over the next few years. Many of these newly discovered heme proteins show the unusual ability to form reversible, intramolecular hexacoordinate complexes. Examples of this group include the carbon monoxide dependent transcription activator CooA, the *Escherichia coli* oxygen sensor EcDos, nonsymbiotic plant hemoglobins (nsHbs), *Chlamydomonas* Hb, *Synechocystis* Hb, and human neuroglobin (*4*, *6*, *8*−*11*). The hexacoordinating amino acid side chain exerts considerable influence on ligand binding to these Hbs. Instead of a simple bimolecular reaction as is observed with traditional pentacoordinate Hbs, ligand binding to hexacoordinate Hbs is a complex competition between the binding of the exogenous ligand and intramolecular coordination by a local amino acid side chain. The large number of newly discovered heme proteins exhibiting this behavior, coupled with wide variation in hexacoordination kinetics, indicates that this is a fundamentally new and ubiquitous method for regulation of ligand binding to heme proteins.

Methods have recently been developed for the kinetic characterization of hexacoordination and ligand binding in hexacoordinate hemoglobins (*12*). These methods were developed using the nsHb from rice (rHb1) in which hexacoordination in the ferric and deoxy ferrous forms results from the binding of a histidine side chain to the sixth coordination site of the heme iron (Figure 1A). When ligand binding is initiated by flash photolysis of the ligand bound protein (Figure 1C), the reaction begins with the protein in the pentacoordinate state (Figure 1B). Under these conditions, rate constants for hexacoordination and bimolecular ligand binding can be determined by monitoring biexponential ligand rebinding (*12*). However, under physiological conditions it is unlikely that ligand binding starts from a completely pentacoordinate population of protein molecules. It is much more likely that the protein exists in an equilibrium mixture of the hexacoordinate and pentacoordinate forms. When a suitable ligand becomes available, the rate of binding would then be determined by the fraction of protein in the pentacoordinate form in conjunction with the rate constants associated with ligand binding and hexacoordination.

The work described here uses rapid mixing and kinetic analysis to investigate the ligand binding reactions of several hexacoordinate hemoglobins. The rate constants for ligand binding and hexacoordination determined by flash photolysis are evaluated against time courses for ligand binding obtained from rapid mixing experiments. These comparisons demonstrate that the simple hexacoordination reaction scheme shown in Figure 1 is not sufficient to fully describe ligand binding to these proteins. A general model describing ligand binding to hexacoordinate hemoglobins is developed that accounts for reactions following rapid mixing and flash photolysis.

† We would like to acknowledge the USDA for support of this work (Award No. 99-35306-7833).

* To whom correspondence should be addressed. Phone: (515) 294-2616; fax: (515) 294-0453; E-mail: msh@iastate.edu.

[1] Abbreviations: Mb, myoglobin (horse heart); Hb, hemoglobin; nsHb, nonsymbiotic plant hemoglobin; rHb1, rice nonsymbiotic plant hemoglobin I; H73L, rice nonsymbiotic plant hemoglobin I mutant with a leucine substituted for the distal coordinating histidine (H73); synHb, *Synechocystis* hemoglobin; ckHb1, *Cichorium* hemoglobin I; msHb, moss hemoglobin (*Physcomitrella*).

10.1021/bi0100790 CCC: $20.00 
Published on Web 04/27/2001

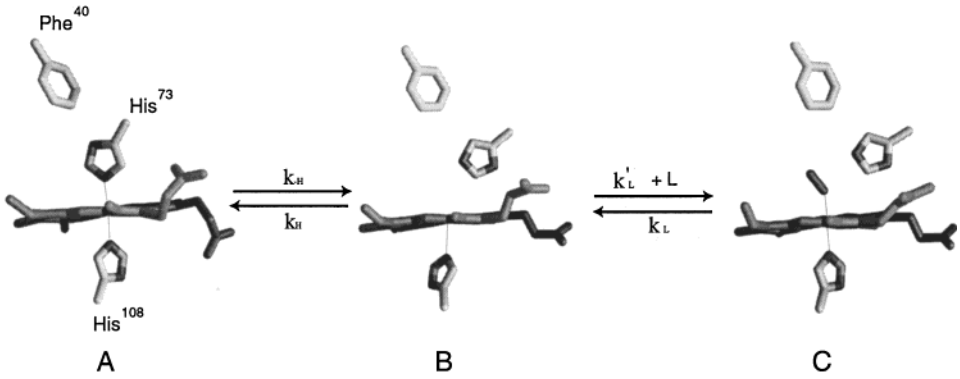


FIGURE 1: Ligand binding to rHb1. (A) The ferrous deoxy form of this protein has a His side chain coordinated to the ligand binding site that must dissociate to form the reactive pentacoordinate species. This heme pocket is that of rHb1 (*10*). (B) The heme pocket of deoxy lupin leghemoglobin (*28*) serves as a model for deoxy rHb1. (C) CO bound lupin leghemoglobin (*29*) serves as a model for the heme pocket of ligand bound rHb1. The rate constant for each of these reactions is titled along with the arrow indicating the reaction. The relative position of the highly conserved phenylalanine side chain is shown in each of the heme pockets.

## MATERIALS AND METHODS

*Bacterial Strains and Culture Conditions.* All of the proteins examined here were obtained through recombinant expression techniques. *E. coli* BL21(λDE3)-CodonPlus-RP cells (*E. coli*-CP-RP) (Stratagene) were used as the protein expression host. These cells were grown in a fermentation apparatus consisting of a 20 L polypropylene carboy resting in a 40 L open rectangular water bath that regulates the growth culture temperature. Aeration was accomplished through mild stirring with a 6-cm magnetic stir bar accompanied with $O_2$ that was bubbled through autoclave durable aquarium air stones at 60 psi. Expression media consisted of Terrific Broth supplemented with 50 μg/mL kanamycin, 50 μg/mL chloramphenicol, and 1.0 mL of antifoam (Sigma).

*Cloning, Expression, and Purification of Recombinant Proteins.* The cDNAs coding for each protein were inserted into pET29a (Novagen) between the NdeI and EcoRI restriction sites in the multicloning region. The rHb1 H73L mutant protein was generated as described previously (*13*). The source of the cDNAs were rHb1 and H73L rHb1 (*13*), synHb (Hvitved et al., unpublished data), ckHb1 (*14*), and msHb (*15*).

Each plasmid was grown in 20 L of the expression media at 37 °C until the optical density at 600 nm was 1.5, at which time expression was induced by the addition of IPTG (Sigma) to a final concentration of 500 μM. In some instances, 5 mg/L hemin chloride (solubilized in 0.1 M NaOH) was added at induction to increase the fraction of soluble protein. However, the addition of hemin chloride was not required for the formation of soluble, heme-bound protein and was not added at later stages of protein purification. Protein expression was allowed to continue for 5 h, followed by harvest of the culture. This was done by formation of a pellet of the cells through centrifugation (∼5000 g for 10 min). The harvested cells and lysis supernatants all displayed bright red color, as typically seen in soluble heme-bound hemoglobins.

All proteins were then purified using a three-stage procedure consisting of ammonium sulfate fractionation, and phenyl-sepharose and DEAE-cellulose column chromatography (*13*). The protein solutions were dialyzed into 20 mM Tris (pH 8.5) after the phenyl-sepharose separation and prior to the DEAE-cellulose purification step. This three stage procedure typically results in proteins with a Soret/$A_{280\ nm}$ ratio > 3.0. Horse heart myoglobin was obtained commercially from Sigma and not subjected to further purification.

Table 1: Absorbance Peaks and Rate Constants[a]

| protein | CO-heme peak (nm) | $k'_{CO}$ ($\mu M^{-1}\,s^{-1}$) ± 10% | $k_O$ ($s^{-1}$) ± 10% | $k_{-O}$ ($s^{-1}$) ± 10% |
|---|---|---|---|---|
| HH Mb | 423 | 0.5 | N/A | N/A |
| rHb1 | 416 | 6.0 | 60 | 600 |
| H73L | 416 | 161 | 80 | 8000 |

[a] The absorbance peaks monitored for each protein during CO binding experiments and CO binding, opening, and closing rate constants. The positions of the CO-heme absorbance peaks in synHb, msHb, and ckH1 are 417, 419, and 419 nm, respectively.

*Kinetic Experiments.* Rapid mixing experiments were carried out with a Durrum stopped flow apparatus interfaced with a personal computer using previously described methods (*16*, *17*). Absorbance spectra were collected during CO binding using an On Line Instruments (OLIS) rapid scanning monochromator (RSM) stopped flow apparatus. Samples were prepared as follows. Perfektum gastight syringes containing 100 mM potassium phosphate (pH 7.0) were bubbled with either CO or $N_2$ for 20 min. Dry sodium dithionite was then added to each syringe to a concentration of ∼200 μM. Solutions of CO prepared in this way are 1000 μM, with lower concentrations of CO obtained through dilution of the 1000 μM solution into secondary syringes containing buffer equilibrated in $N_2$. The protein sample syringe consisted of $N_2$ equilibrated buffer with ∼200 μM sodium dithionite and ∼1 μM protein. Reactions were monitored at the corresponding CO-bound heme absorbance maximum for each protein sample as listed in Table 1.

*Data Analysis.* Rate constants for CO binding to rHb1 were extracted from least-squares fits to binding time courses between 0.003 s (the dead time of the stopped flow apparatus) and 0.2 s. Below [CO] of 50 μM, a two exponential decay expression was necessary to describe the time courses (Figure 4). The faster of these rate constants are shown in Figure 5A (filled circles), and the slower are shown in Figure 5A (open circles) and Figure 6A. Above 50 μM [CO], data between 0 and 200 ms fit well to a single-exponential decay (Figure 4C).

The H73L rHb1 rate constants were determined using single-exponential fits to the rapid-mixing time courses

Table 2: Percentages of Each Fraction of CO Binding Following Rapid Mixing[a]

| protein | open fraction (%) | closed fraction *fast* (%) | closed fraction *slow* (%) |
|---|---|---|---|
| rHb1 | 30 | 50 | 20 |
| msHb | 10 | 20 | 70 |
| ckHb1 | 20 | 30 | 50 |
| synHb | | 80 | 20 |
| H73L | | 75 | 25 |

[a] The relative percentage associated with each fraction of CO binding to the hexacoordinate hemoglobins in Figure 2A. These fractions were determined using reactions at 30 $\mu$M [CO]. H73L and synHb exhibit only the slower fractions because binding to the open fraction is lost in the dead time of the reaction (Hvitved et al., unpublished).

between 0.003 and 0.2 s at [CO] less than 50 $\mu$M. At concentrations above 50 $\mu$M [CO], data were fit to a double exponential expression and the faster rate constants interpreted in Figure 7 along with the single-exponential fits for the time at [CO] < 50 $\mu$M. The presence of a second rate constant in the higher [CO] time courses was attributed to the slower binding phenomenon demonstrated in Figures 2 and 3, which is the subject of ongoing investigation. Selected rate constants are listed in Table 1. The kinetic simulation in Figure 6B was generated using the program KINSIM (*18*). All graphic representations and data analysis were carried out using the program Igor Pro (Wavemetrics, Inc).

## RESULTS

*Time Courses for Ligand Binding Following Rapid Mixing.* The reaction scheme for hexacoordination shown in Figure 1 can be simplified to the following equation if the dissociation rate constant for the bound ligand is very small as compared to all other rate constants, and the reaction is carried out under pseudo first order conditions with the ligand in excess. On the basis of this equation and using an

$$\mathrm{Hb_H} \underset{k_{\mathrm{H}}}{\overset{k_{-\mathrm{H}}}{\rightleftharpoons}} \mathrm{Hb_P} \xrightarrow{k'_{\mathrm{L}}[\mathrm{L}]} \mathrm{Hb_L} \qquad (1)$$

improved steady-state approximation for $Hb_P$ (*19*), the following equation can be derived for the observed rate constant of ligand binding following rapid mixing.

$$k_{\mathrm{obs,H}} = \frac{k_{-\mathrm{H}} k'_{\mathrm{L}}[\mathrm{L}]}{k_{-\mathrm{H}} + k_{\mathrm{H}} + k'_{\mathrm{L}}[\mathrm{L}]} \qquad (2)$$

Equation 2 predicts a single-exponential decay time course that is dependent upon the concentration of the ligand. However, if $k'_{\mathrm{L}}[\mathrm{L}] \gg k_{-\mathrm{H}} + k_{\mathrm{H}}$, the observed rate of reaction will be $k_{-\mathrm{H}}$ regardless of the ligand concentration (*20*).

Rapid mixing time courses for carbon monoxide binding to several hexacoordinate hemoglobins are shown in Figure 2A along with horse heart myoglobin (Mb) for comparison. Unlike the hexacoordinate hemoglobins, Mb is strictly pentacoordinate in the reduced, unligated form and its time course fits well to a single-exponential decay. However, none of the hexacoordinate hemoglobin time courses fit well to single-exponential terms. This disagrees with the behavior predicted by eq 2 and indicates that ligand binding following rapid mixing is more complex than the reaction shown in Figure 1 and described by eq 1. The various hexacoordinate hemoglobins exhibit differing degrees of divergence from single-exponential binding, with the most extreme deviance displayed by the nsHb from moss.

To rule out slow drifts in absorbance or slow equilibration of the final absorbance spectra as the cause of nonideality in Figure 2A, complete spectra were measured during CO binding using a rapid scanning stopped flow apparatus. An example of these spectra is given in Figure 2B for CO binding to synHb. All reactions exhibited discrete isosbestic points, demonstrating that the only reaction occurring on these time scales is the conversion of deoxy Hb to CO bound Hb.

The time course for CO binding to rHb1 at low [CO] (10 $\mu$M) is examined in more detail in Figure 3. The fitted curves in this figure have been isolated to demonstrate graphically the different fractions of binding present in the time course. Thus, the fitted curve in Figure 2A for rHb1 represents the sum of the fitted curves presented in Figure 3. Of these three distinct fractions of ligand binding, two exist in the 0 to 200 ms region and can be described with single exponential terms. The third fraction of rebinding occurs on a much slower time scale and is heterogeneous in nature, unable to be described with a single exponential fit. The percent of ligand binding that occurs in each fraction for rHb1 is listed in Table 1. As the majority of binding to rHb1 occurs during the first 200 ms, our current effort to model ligand binding concerns only these two phases of binding. The slow binding, heterogeneous fraction (that occurring after 200 ms) will be analyzed later in the context of a hexacoordinate hemoglobin that exhibits a large amount of rebinding during this time.

Figure 4 demonstrates that two exponential terms are necessary for fitting CO binding to rHb1 at low [CO] (<50 $\mu$M). Figure 4A is a time course for CO binding to rHb1 at 20 $\mu$M [CO]. Single and double exponential decays were fit by least squares to this time course and are shown along with the raw data. Residuals from each fit are shown in Figure 4B. In this case, the fit to the double exponential decay provides a significantly better model than the single-exponential decay. At [CO] > 50 $\mu$M, a single exponential decay successfully accounts for all binding amplitude on this time scale. Figure 4C demonstrates this with a time course for CO binding to rHb1 at 400 $\mu$M [CO]. Single and double exponential decays were fit to the time course and overlaid with the raw data. The residuals for each fitted curve are plotted above the time course. In this case, no benefit is derived from inclusion of a second exponential when fitting the time course, as the residuals from the two fits are functionally identical. These results indicate that the more rapid rate constant for binding in Figure 4A is lost in the mixing dead time (~0.003 s) at the higher [CO] giving rise to Figure 4C.

*Comparison of $k_{obs,H}$ by Flash Photolysis and Rapid Mixing.* Equation 2 predicts a single exponential binding event if the reaction in eq 1 is at rapid equilibrium. The rHb1 rate constants for each of the terms in eq 2 have been measured independently using flash photolysis and are 1911 $s^{-1}$, 517 $s^{-1}$, and 6.0 $\mu M^{-1}$ $s^{-1}$ for $k_{-\mathrm{H}}$, $k_{\mathrm{H}}$, and $k'_{\mathrm{CO}}$, respectively (*12*). Therefore, the [CO] dependence of $k_{\mathrm{obs,H}}$ predicted from eq 2 can be compared to that of the two rate constants extracted from the 0−200 ms time courses for binding following rapid mixing.

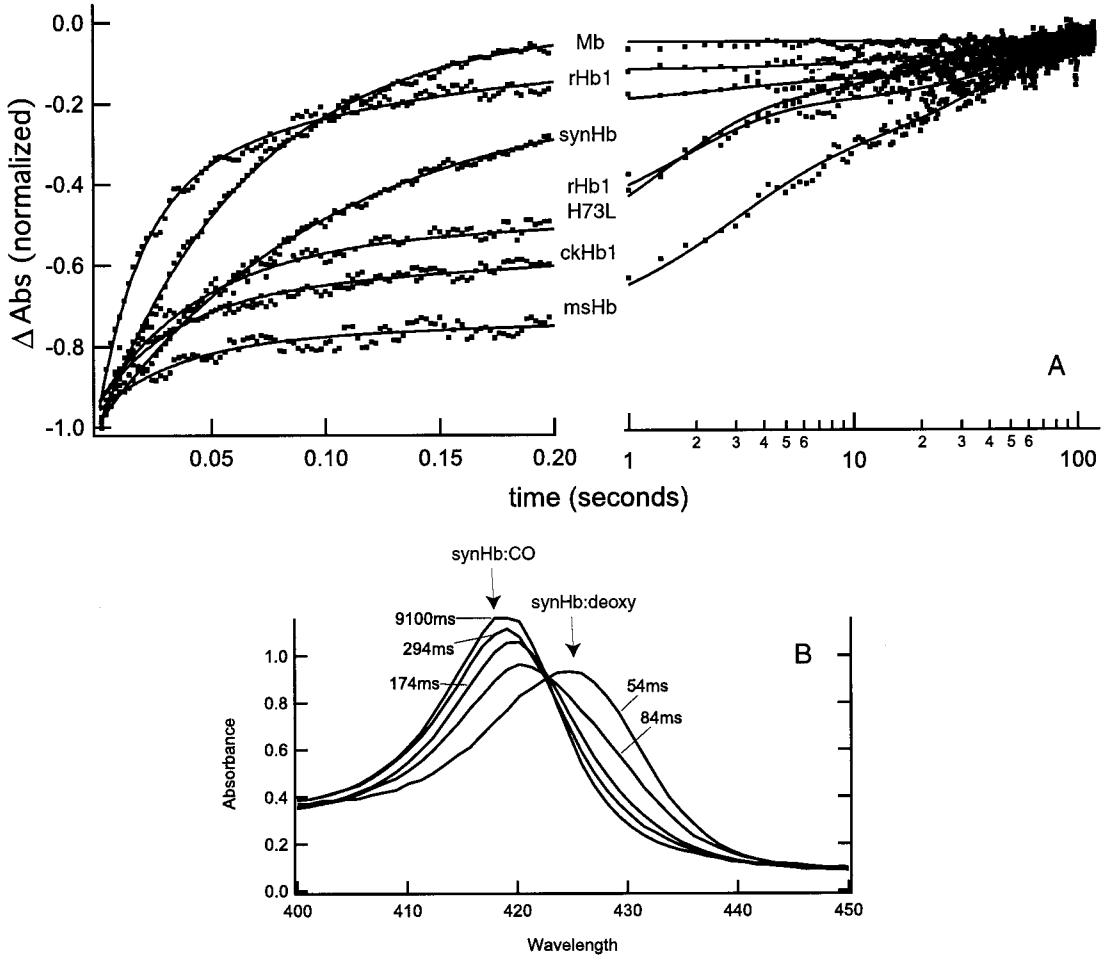


FIGURE 2: CO binding time courses for several hexacoordinate hemoglobins and myoglobin. (A) The change in absorbance at the CO-heme absorbance peak following rapid mixing of each protein at 30 $\mu$M [CO] is plotted against time. To facilitate comparison, the time axis is linear for the first 200 ms and log scale for the remainder. The fitted curves are a single-exponential fit for Mb, double exponential fits for synHb and H73L rHb1, and three exponentials fits for the rest. This figure serves to illustrate the diversity and heterogeneity in ligand binding exhibited by hexacoordinate hemoglobins. (B) Absorbance spectra following rapid mixing of synHb at 30 $\mu$M [CO]. Individual spectra are labeled with their time of acquisition following the rapid mixing event. This figure demonstrates a single transition from the deoxy protein to the CO bound form.

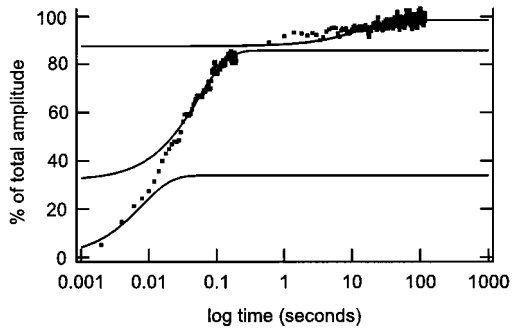


FIGURE 3: Different fractions of ligand binding to rHb1. This is a time course for CO binding to rHb1 at 30 $\mu$M [CO]. The three exponential fitted curve has been partitioned into its component single-exponential fitted curves, which are overlaid on corresponding regions of the time course. The bottom curve represents the open fraction, the middle curve is the faster of the "closed" fractions, and the top curve shows the heterogeneous, "slow" fraction of ligand binding. Fractions of binding resulting from fits to the other hexacoordinate hemoglobins in Figure 2A are given in Table 2.

This comparison is shown in Figure 5A with the expected values of $k_{obs,H}$ predicted from eq 2 shown as a line, the faster of the two rapid mixing rate constants shown as filled circles, and the slower as open circles. The faster of the two rate constants (filled circles) is lost in the mixing dead time at [CO] > 50 $\mu$M. Another comparison of the CO binding predicted from eq 2 and that observed following rapid mixing is shown in Figure 5B. A simulated time course for CO binding (400 $\mu$M) to rHb1 following rapid mixing was generated using the mechanism in eq 1 and the rate constant calculated from eq 2. Figure 5B illustrates the poor correlation between this simulation and the corresponding experimentally acquired time course.

There are two important points made in Figure 5. (i) CO binding following rapid mixing is more complex than what is predicted from eqs 1 and 2. (ii) The faster of the two observed rate constants corresponds with the predicted rate constant from eq 2. Thus rHb1 exists in a mixture of states, with a fraction of the protein behavior described by eqs 1 and 2. As shown in Table 2, this fraction comprises approximately 30% of binding to rHb1. Evidently this population of molecules exists in rapid equilibrium between $Hb_H$, and $Hb_P$, behaving in accordance with the mechanism shown in Figure 1.

This suggests that the remaining 70% of rHb1 molecules exist as a discrete population, indicating that the overall binding reaction is not at rapid equilibrium and must therefore contain a slowly reacting species. We have defined

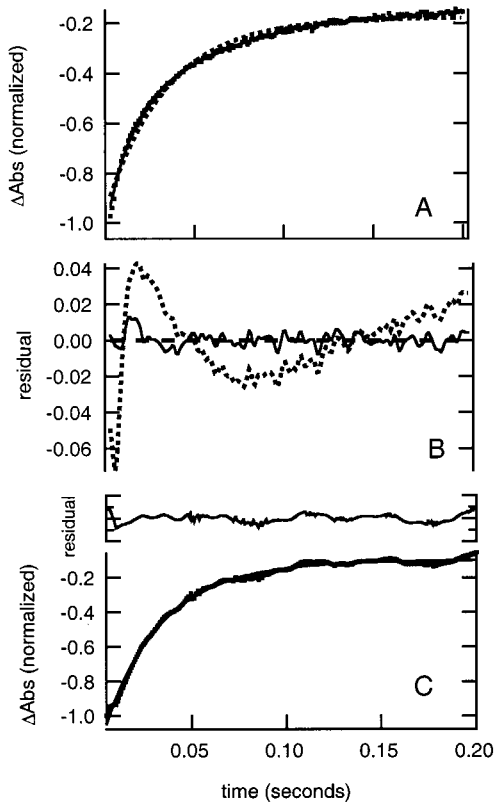


FIGURE 4: Time courses for CO binding to rHb1 at high and low [CO]. (A) A time course for CO binding to rHb1 at 20 $\mu$M [CO]. The data are plotted along with double (solid line) and single (dotted line) exponential fits to the time course. (B) Residuals from the single (dotted line) and double (solid line) exponential fits from (A). (C) CO binding to rHb1 at 400 $\mu$M [CO]. As in panel A, the data were fit to single (dashed line) and double (solid line) exponential expressions. The residuals from each fit are plotted above the time course. These data illustrate that time courses below 50 $\mu$M [CO] are biphasic on this time scale. At [CO] > 50 $\mu$M, the time courses are monophasic.

the population not described by the reaction in eq 1 to be a "closed" form of the protein. In rHb1, CO binding to the majority of the closed protein (50% of total binding) is relatively rapid and dependent on ligand concentration. The remaining fraction of closed protein (20% of total binding) is the slow binding, heterogeneous phase mentioned above. To avoid confusion, the two fractions of closed protein are referred to respectively as "closed-fast binding" and "closed-slow binding," with the term "closed" indicating the sum of the two.

*A Model for Ligand Binding.* There are two realistic models that could explain this closed population of protein. (i) Hexacoordination by His[73] is heterogeneous and results in two phases of ligand binding. (ii) The closed form of the protein involves a conformation that must shift to an "open" form (that associated with the 30% binding corresponding with Figure 1 and eq 2) prior to His[73] dissociation and formation of the reactive pentacoordinate species. The time courses for hexacoordination and ligand binding following flash photolysis are exactly those expected for a mechanism comprising a single hexacoordinating species (*12*). Furthermore, the structure of rHb1 suggests a homogeneous hexacoordinate conformation (*10*). With no support for heterogeneous hexacoordination, the latter of the two models was selected as a hypothesis for ligand binding to rHb1.

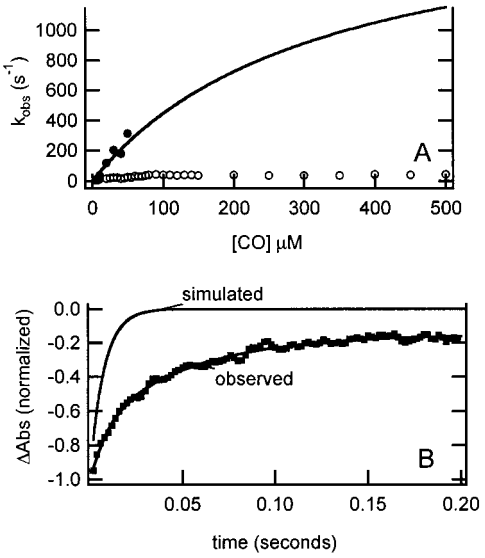


FIGURE 5: A comparison of rate constants for rapid mixing to those predicted from the individual rate constants for hexacoordination. (A) The fast (filled circles) and slow (open circles) rate constants obtained from the double exponential fits to the time courses for CO binding to rHb1 are shown as a function of [CO]. The faster of the two observed rate constants becomes immeasurable at [CO] > 50 $\mu$M due to the mixing dead time. The predicted values of $k_{obs,H}$ from eq 2 are simulated as a function of [CO] and shown as a solid line. There is a very good correlation between the faster of the two observed rate constants and the values associated with hexacoordination and bimolecular ligand binding. (B) A time course resulting from rapid mixing of rHb1 at 400 $\mu$M [CO] (squares) is plotted with its single-exponential fitted curve (solid line running through the data points) and a simulated data trace predicting rHb1 binding at 400 $\mu$M in accordance with eq 2. A clear difference exists between the predicted and observed time courses.

Equation 3 describes this kinetic mechanism:

$$\mathrm{Hb_C} \underset{k_{-O}}{\overset{k_O}{\rightleftharpoons}} \mathrm{Hb_{O,H}} \underset{k_H}{\overset{k_{-H}}{\rightleftharpoons}} \mathrm{Hb_{O,P}} \xrightarrow{k'_L[L]} \mathrm{Hb_{O,L}} \qquad (3)$$

$Hb_C$ is the closed form of the protein; $Hb_{O,H}$ is the open hexacoordinate form (corresponding with Figure 1A); $Hb_{O,P}$ is the open pentacoordinate form (corresponding with Figure 1B); and $Hb_{O,L}$ is the open ligand-bound form of the protein (corresponding with Figure 1C). Since $Hb_C$ is not at rapid equilibrium with the open forms of the protein, the rate constant for opening ($k_O$) must be slow in comparison with the rate constants for hexacoordination and bimolecular ligand binding. Under these conditions, ligand binding following flash photolysis will involve only the open forms of the protein, and ligand binding following rapid mixing will be heterogeneous. This interpretation is in agreement with both the data presented here (Figure 2) and that determined previously from flash photolysis (*12*).

*Kinetic Analysis of $Hb_C$.* Equation 3 can be used in combination with steady-state approximations for $Hb_{O,H}$ and $Hb_{O,P}$ to calculate the observed rate constant for ligand binding to $Hb_C$ following rapid mixing.

$$k_{obs,C} = \frac{k_{-H}k_O k'_L[L]}{k_H k_{-O} + k_O[k_{-H} + k_H] + [k_O + k_{-O} + k_{-H}]k'_L[L]} \qquad (4)$$

In this equation, each rate constant is defined as in eq 3.

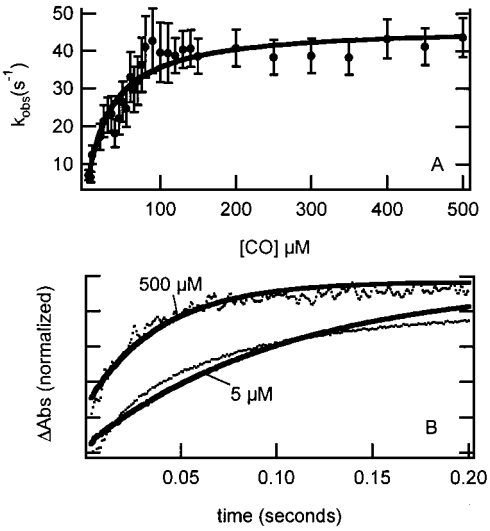


FIGURE 6: The concentration dependence of CO binding to "closed" rHb1. (A) The slower rate constant for CO binding in Figure 5A is shown again here with the ordinate axis scaled appropriately. Each data point is an average of several replications of rapid mixing experiments at each concentration of CO. Error bars are the variance in each data point. The solid line is a least-squares fit for $k_O$ and $k_{-O}$ in eq 4 with values for $k_{-H}$, $k_H$, and $k'_{CO}$, fixed at 1911 $s^{-1}$, 517 $s^{-1}$, and 6.0 $\mu M^{-1}$ $s^{-1}$, respectively (*12*). The fitted values for $k_O$ and $k_{-O}$ are 60 and 600 $s^{-1}$, respectively. (B) The program KINSIM4.0 was used to generate simulated time courses for rHb1 rapid mixing at [CO] of 500 and 5 $\mu$M according to the mechanism described by eq 3. The corresponding experimentally acquired time courses at the same concentrations were then normalized and plotted within this figure. This indicates that a more accurate description of binding is provided by eq 3 as compared to that of eq 1 (Figure 5B).

Similar to eq 2, eq 4 predicts concentration-dependent ligand binding unless $k_O$ is very small in comparison to the other rate constants. Under these circumstances, the limiting value of $k_{obs,C}$ will be exactly equal to $k_O$.

To test the model described in eq 3, the dependence of $k_{obs,C}$ on CO concentration was measured. These data are shown in Figure 6A. Because $k_{obs,C}$ approaches an asymptote, it was possible to extract values for the rate constants $k_O$ and $k_{-O}$ from a least-squares fit to eq 4 with $k_{-H}$, $k_H$, and $k'_L$ fixed at the values previously determined by flash photolysis. The fitted values for $k_O$ and $k_{-O}$ are 60 and 600 $s^{-1}$, respectively.

Using these values and the rate constants determined from flash photolysis, numerical integration of the kinetic scheme in eq 3 was used to simulate rapid mixing time courses for CO binding to rHb1. Figure 6B shows simulated time courses for CO binding at concentrations of 5 and 500 $\mu$M along with the corresponding observed time courses. The correlation between the simulated and observed traces at high and low [CO] in Figure 6B is in sharp contrast to Figure 5B, demonstrating the ability of the model in eq 3 to predict CO binding to rHb1 with greater accuracy than the model in eq 1.

The values of $k_O$ and $k_{-O}$ measured for rHb1 predict an equilibrium constant for opening, $K_O$ ($k_O/k_{-O}$), of 0.1. Our analysis of this reaction scheme and the fitted values for $k_O$ and $k_{-O}$ can be tested by comparing this kinetically determined value of $K_O$ with the equilibrium value calculated from the fraction of protein which exists in the closed form (Table 2). The relationship between the fraction of closed protein and $K_O$ is derived beginning with eq 5, which defines $\gamma_c$ as the fraction of protein in the closed form prior to rapid mixing. When the concentration of each species in eq 5 is

$$\gamma_C = \frac{Hb_C}{Hb_{O,P} + Hb_{O,H} + Hb_C} \quad (5)$$

normalized to $Hb_{O,P}$, the following equilibrium relationships exist; $Hb_{O,P} = 1$, $Hb_{O,H} = K_H$, and $Hb_C = K_H/K_O$ (where $K_H$ is $k_H/k_{-H}$). Solving for $K_O$ yields the following relationship between $K_O$ and $\gamma_c$:

$$K_O = \frac{K_H(1 - \gamma_c)}{\gamma_c(1 + K_H)} \quad (6)$$

Applying eq 6 to rHb1 [$\gamma_c = 0.7$ ($\pm$ 10%); Table 1] with $K_H$ determined from flash photolysis [$K_H = k_H/k_{-H} = 0.3$ ($\pm$ 10%)] results in a value for $K_O$ of 0.1 ($\pm$ 10%). This provides equilibrium corroboration of our kinetically determined value of $K_O$, and further supports the model proposed in eq 3.

*Determination of the Necessity of Hexacoordination in the Formation of Hb$_C$.* To investigate whether the closed protein form is contingent upon hexacoordination, ligand binding was measured using a pentacoordinate mutant rHb1 protein in which $His^{73}$ was replaced with Leu (H73L rHb1). This protein has previously been shown to be pentacoordinate and has a very rapid bimolecular rate constant for CO binding following flash photolysis ($k'_{CO}$ = 161 $\mu M^{-1}$ $s^{-1}$) (*12*, *13*).

If ligand binding to H73L rHb1 was a simple bimolecular event like that of traditional pentacoordinate hemoglobins, the rapid mixing reaction would be finished in the mixing dead time at [CO] > 5 $\mu$M. However, binding to H73L rHb1 is observed for as long as 100 s at much higher [CO] (Figure 2). This implies that hexacoordination is not required for formation of $Hb_C$.

As the H73L rHb1 mutant protein is capable of existing in a closed conformation and yet incapable of hexacoordination, the following reaction scheme serves to describe ligand binding to this protein.

$$Hb_C \underset{k_{-O}}{\overset{k_O}{\rightleftharpoons}} Hb_{O,P} \xrightarrow{k'_L[L]} Hb_L \quad (7)$$

Equation 7 is of the same form as eq 1, and using a steady-state approximation for $Hb_{O,P}$ provides a similar relationship between $k_{obs}$ and the rate constants for opening and closing in the H73L rHb1 mutant protein. Rate constants for opening

$$k_{obs,H73L} = \frac{k_{-O}k'_L[L]}{k_{-O} + k_O + k'_L[L]} \quad (8)$$

and closing in H73L rHb1 were determined from the concentration dependence of $k_{obs,H73L}$ on the binding of CO following rapid mixing. These data are shown in Figure 7 along with a nonlinear least-squares fit to eq 8 with $k'_L$ = 161 $\mu M^{-1}$ $s^{-1}$. The resulting values of $k_O$ and $k_{-O}$ for H73L rHb1 are 80 and 8000 $s^{-1}$, respectively.

*Ligand Binding to other Hexacoordinate Hemoglobins.* The amplitudes for the three fractions of binding extracted

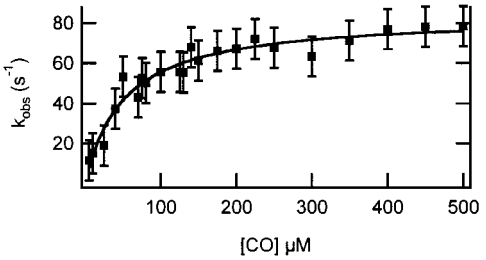


FIGURE 7: The concentration dependence of CO binding to H73L rHb1. Each data point is an average of several replications of rapid mixing experiments at each concentration of CO, and the error bars are the variance in each data point. The solid line is a least-squares fit for $k_O$ and $k_{-O}$ in eq 8 with $k'_{CO}$ fixed 161 $\mu M^{-1}$ $s^{-1}$ (*12*). The values of $k_O$ and $k_{-O}$ extracted from this fit were 80 and 8000 $s^{-1}$, respectively.

from each time course in Figure 2A are reported in Table 1. The percent of total ligand binding that occurs in each fraction varies widely among the hexacoordinate hemoglobins. Binding of CO to synHb and H73L rHb1 on the <200 ms time scale can be described by single-exponential values because binding to the open fraction is lost in the dead time associated with rapid mixing (*12*) (Hvitved et al., unpublished data). Therefore, no "open" fraction binding is reported.

## DISCUSSION

Structural and kinetic investigations of pentacoordinate hemoglobins have been carried out for decades. The resulting mechanisms for ligand binding to these proteins indicate that the distal heme pocket uses specific amino acid side chains to stabilize the ferrous heme iron against oxidation and to create an electrostatic environment appropriate for ligand binding and selectivity (*21*). The use of reversible intramolecular hexacoordination to regulate ligand binding is a more recent discovery and is now known to exist in a large and phylogenetically diverse group of proteins.

The ligand binding model presented here is undoubtedly applicable to many of these hexacoordinate hemoglobins. In demonstration of this, we discuss two hexacoordinate hemoproteins that have been previously investigated; the nsHb from barley, and an oxygen-sensing heme protein (EcDos) from *E. coli* (*9*, *22*). Barley nsHb and rHb1 share significant sequence homology and would be expected to have similar rate constants for ligand binding. However, in contrast to the bimolecular rate constant for CO binding to rHb1 (6 $\mu M^{-1}$ $s^{-1}$), the barley rate constant has been reported as 0.57 $\mu M^{-1}$ $s^{-1}$ (*22*). This value was estimated from stop flow measurements at low [CO]. Values of $k'_{CO}$ were estimated from the slope of $k_{obs}$ at low [CO] with the assumption that this CO concentration range provided a direct measurement of bimolecular binding. Equation 2 (and eq 4) demonstrates that this cannot be the case. When we examine the data for CO binding to rHb1 in Figure 6A with the same methods used by Duff et al. (*22*), we find a similar value of 0.58 $\mu M^{-1}$ $s^{-1}$. Flash photolysis experiments have shown that this does not represent the true value of $k'_{CO}$ (*12*).

EcDos, the oxygen-sensing heme protein from *E. coli* described by Delgado-Nixon et al. (*9*) is also hexacoordinate although it is predicted to be a PAS protein instead of a globin. This protein shows slow and remarkably similar binding rates for $O_2$, CO, and NO when these reactions are initiated by rapid mixing. It is probable that these experiments are not measuring ligand binding that occurs according to a mechanism like that described in eqs 1 and 2. Instead, it is likely they are measuring the reactions described in eqs 3 and 4, with the "opening" event limiting the observed rate of reaction. This hypothesis would explain the very unusual, ligand-independent kinetic binding constants that have been reported. To determine the validity of this hypothesis, the rate constants reported from stopped flow experiments should be compared with values determined from laser flash photolysis. The model presented here resolves the unexpected discrepancy of different ligand binding rates displayed by two very similar nsHbs and also supplies a possible explanation for the unusual ligand binding behavior of Dos.

*Structural Determinants of Heterogeneous Ligand Binding.* Hexacoordinate hemoglobins exist in at least two different states. The term "open" has been applied to the conformation of the protein that is capable of reversible hexacoordination, formation of a pentacoordinate complex, and ligand binding. A "closed" conformation has been attributed to the fraction of protein that reacts more slowly following rapid mixing. In this model, the closed conformation is incapable of ligand binding. The open and closed forms of the hexacoordinate hemoglobins examined here are not at rapid equilibrium on the time scales during which ligand binding is traditionally measured.

A conversion between the two forms of the protein may involve structural rearrangement. The structure of ferric rHb1 when compared with leghemoglobin suggests that folding of the rHb1 D helix region could accompany E helix rearrangement following ligand binding (*10*). It is possible that this reorganization in structure is linked to the slow conformational change observed here. As mentioned before, the crystal structure of rHb1 shows little heterogeneity in hexacoordination and, with the exception of the D helix region, is fairly well ordered. It is possible that the crystal lattice preferentially stabilizes only one conformation of the protein. Structures of ligand-bound and ferrous rHb1 will undoubtedly improve our understanding of the structural role in heterogeneous ligand binding.

Surprisingly, hexacoordination is not required for formation of the closed protein conformation. If this were the case, ligand binding to H73L rHb1 following rapid mixing would be extremely fast and not measurable on conventional stopped flow time scales. Figure 2 and Table 2 demonstrate that this is not the case for at least part of the binding reaction. These results suggest that the differences between open and closed conformations involve structural movement by the polypeptide backbone and are not simply a consequence of a well positioned distal His side chain. Therefore, this conformational change could confer regulation of ligand binding in concert with hexacoordination. It is also possible that ligand binding is predominately regulated by varying the ratio of open and closed fractions of protein. A great deal of regulatory control over ligand binding is possible through a combination of reversible hexacoordination and variation in fractions of open and closed protein.

Additional evidence supporting folding instead of hexacoordination in the regulation of open and closed conformations comes from the fact that the ratios of the closed fractions for rHb1 and H73L are the same (Table 2). In both proteins, ~75% of the closed fraction is fast and monoexponential (closed-fast binding). Future work should inves-

tigate whether the same phenomenon occurs with the moss protein, where the closed-fast binding fraction is much smaller (20%; Table 2).

*Physiological Significance of Hexacoordination.* Traditional pentacoordinate hemoglobins have presumably evolved to bind ligands rapidly (i.e., $>100$ $s^{-1}$ in air) due to their roles in oxygen transport and scavenging. To optimize this function myoglobins and mammalian hemoglobins have developed rigid, "open" heme pocket conformations that create minimal resistance to entering ligands. Regulation of overall affinity is thus a function of the electrostatic environment in the heme pocket and the innate reactivity of the heme iron (which can be affected by electrostatics and proximal coordination) (*21*, *23*). These biophysical properties vary among hemoglobins and are tailored to the specific physiological needs of the organism. For example, the oxygen affinity of human hemoglobin is highly regulated for proper transfer between the lungs and other tissues. In plant leghemoglobins, the affinity and kinetics of the reaction with oxygen are ideally suited for the unique function of scavenging and delivery required during symbiotic nitrogen fixation (*24*). It is probable that both reversible hexacoordination and slow conformational changes are linked to physiological function in the hexacoordinate hemoglobins.

There are two fundamental possibilities for the relationship of hexacoordination and slow conformational changes to physiological function. (i) These reactions may exist to regulate the biochemical reactivity of hexacoordinate hemoglobins. (ii) Hexacoordination and conformational changes may be moderators in a signal transduction response. These two possibilities are not mutually exclusive. In support of the first possibility are the unique properties of nsHbs. These proteins have unusually low oxygen dissociation rate constants in combination with moderately rapid bimolecular association rate constants. They also discriminate unusually well against the binding of CO in favor of oxygen (*25*). It is possible that these properties are a result of hexacoordination and slow conformational changes.

Support for the second possibility comes from work demonstrating that rHb1 quaternary structure is affected by ligand binding (*26*). Furthermore, the discovery of hemoglobins with catalytic domains solidifies the potential for involvement in signal transduction pathways (*7*). These "heme-based sensors" may serve to coordinate an organism's response to varying levels of a number of possible heme ligands. The ligand binding heterogeneity reported here indicates that different fractions of protein are present at the same time. As these forms are differentially reactive, changes in $K_O$ could regulate the fraction of protein present in an "active" form. The variability in $K_O$ observed for the different hexacoordinate hemoglobins may reflect the different responses required by each organism to a particular ligand. Slow conformational regulation has been demonstrated in other protein systems. One example bearing similarity to the mechanism proposed here is the kinetic model describing ligand binding to bacterial histidine permease (*27*). In this system, the histidine binding protein HisJ can exist in different conformations, altering histidine transport dynamics.

The number and diverse nature of organisms containing hexacoordinate hemoglobins suggest these proteins serve important roles in all living creatures. The complexity in their mechanism of ligand binding indicates that their reactivity has the potential for a large degree of regulation. A thorough understanding of these reactions in a number of different hemoglobins will be invaluable for correlating biophysical and physiological function. The model presented here provides a mechanistic basis on which to build an understanding of the structure and function of this class of hemoglobins.

## ACKNOWLEDGMENT

We thank Drs. Cyril Appleby and John S. Olson for careful readings of this manuscript and many helpful suggestions. We also appreciate the use of the rapid scanning stopped flow spectrophotometer in the laboratory of Dr. James Espenson at Iowa State University.

## REFERENCES

1. Hou, S., Larsen, R., Boudko, D., Riley, C., Zimmer, K., Ordal, G., and Alam, M. (2000) *Nature 403*, 540−544.
2. Couture, M., Yeh, S., Wittenberg, B. A., Wittenberg, J. B., Ouellet, Y., Rousseau, D. L., and Guertin, M. (1999) *Proc. Natl. Acad. Sci. U.S.A. 96*, 11223−11228.
3. Scott, N., and Lecomte, J. (2000) *Protein Sci. 3*, 587−597.
4. Couture, M., Das, T. K., Lee, H. C., Peisach, J., Rousseau, D. L., Wittenberg, B. A., Wittenberg, J. B., and Guertin, M. (1999) *J. Biol. Chem. 274*, 6898−6910.
5. Arredondo-Peter, R., Hargrove, M. S., Moran, J. F., Sarath, G., and Klucas, R. V. (1998) *Plant Physiol. 118*, 1121−1125.
6. Burmester, T., Welch, B., Reinhardt, S., and Hankeln, T. (2000) *Nature 407*, 520−523.
7. Rodgers, K. R. (1999) *Curr. Opin. Chem. Biol. 3*, 158−167.
8. Lanzilotta, W., Schuller, D., Thorsteinsson, M., Kerby, R., Roberts, G., and Poulos, T. (2000) *Nat. Struct. Biol. 10*, 876−880.
9. Delgado-Nixon, V., Gonzalez, G., and Gilles-Gonzalez, M. (2000) *Biochemistry 39*, 2685−2691.
10. Hargrove, M., Brucker, E., Stec, B., Sarath, G., Arredondo-Peter, R., Klucas, R., Olson, J., and Phillips, G. (2000) *Structure Fold. Des. 8*, 1005−1014.
11. Couture, M., Das, T., Savard, P., Ouellet, Y., Wittenberg, J., Wittenberg, B., Rousseau, D., and Guertin, M. (2000) *Eur. J. Biochem. 267*, 4770−4780.
12. Hargrove, M. (2000) *Biophys. J. 79*, 2733−2738.
13. Arredondo-Peter, R., Hargrove, M. S., Sarath, G., Moran, J. F., Lohrman, J., Olson, J. S., and Klucas, R. V. (1997) *Plant Physiol. 115*, 1259−1266.
14. Hendriks, T., Scheer, I., Quillet, M. C., Randoux, B., Delbreil, B., Vasseur, J., and Hilbert, J. L. (1998) *Biochim. Biophys. Acta 1443*, 193−197.
15. Arredondo-Peter, R., Ramirez, M., Sarath, G., and Klucas, R. V. (2000) *Plant Physiol. 122*, 1458.
16. Olson, J. (1981) *Methods Enzymol. 76*, 631−651.
17. Hargrove, M. S., Barry, J. K., Brucker, E. A., Berry, M. B., Phillips, Jr., G. N., Olson, J. S., Arredondo-Peter, R., Dean, J. M., Klucas, R. V., and Sarath, G. (1997) *J. Mol. Biol. 266*, 1032−1042.
18. Barshop, B. A., Wrenn, R. F., and Frieden, C. (1983) *Anal. Biochem. 130*, 134−142.
19. Espenson, J. (1995) *Chemical Kinetics and Reaction Mechanisms*, McGraw-Hill, New York.
20. Coletta, M., Angeletti, M., De Sanctis, G., Cerroni, L., Giardina, B., Amiconi, G., and Ascenzi, P. (1996) *Eur. J. Biochem. 235*, 49−53.
21. Olson, J., and G. J. Phillips. (1997) *J. Biol. Inorg. Chem. 2*, 544−552.
22. Duff, S. M. G., Wittenberg, J. B., and Hill, R. D. (1997) *J. Biol. Chem. 272*, 16746−16752.
23. Dickerson, R. E., and Geis, I. (1983) *Hemoglobin: Structure, Function, Evolution, and Pathology*, Benjamin/Cummings Publishing Company, Menlo Park.

24. Appleby, C. A. (1984) *Annu. Rev. Plant Physiol. 35*, 443−478.
25. Trevaskis, B., Watts, R. A., Andersson, C. R., Llewellyn, D. J., Hargrove, M. S., Olson, J. S., Dennis, E. S., and Peacock, W. J. (1997) *Proc. Natl. Acad. Sci. U.S.A. 94*, 12230−12234.
26. Goodman, M., and Hargrove, M. (2001) *J. Biol. Chem. 276*, 6834−6839
27. Wolf, A., Lee, K., Kirsch, J., and Ames, G. (1996) *J. Biol. Chem. 271*, 21243−21250.
28. Harutyunyan, E. H., Safonova, T. N., Kuranova, I. P., Popov, A. N., Teplyakov, A. V., Obmolova, G. V., Rusakov, A. A., Vainshtein, B. K., Dodson, G. G., and Wilson, J. C. (1995) *J. Mol. Biol. 251*, 104−115.
29. Harutyunyan, E. H., Safonova, T. N., Kuranova, I. P., Popov, A. N., Teplyakov, A. V., Obmolova, G. V., Valnshtein, B. K., Dodson, G. G., and Wilson, J. C. (1996) *J. Mol. Biol. 264*, 152−61.

BI0100790